ELSEVIER

Journal of Nuclear Materials 313–316 (2003) 539–542

journal of nuclear materials

www.elsevier.com/locate/jnucmat

Supersonic gas injection on Tore Supra

B. Pégourié [a,*], E. Tsitrone [a], R. Dejarnac [a], J. Bucalossi [a], G. Martin [a], J. Gunn [a], D. Frigione [b], D. Reiter [c], P. Ghendrih [a], C. Clément [a]

[a] *Euratom Association – CEA sur la Fusion Contrôlée, Centre d'Etude de Cadarache, F-13108 Saint Paul Lez Durance cedex, France*

[b] *Centro Ricerche – ENEA CP 65, 00044 Frascati, Roma, Italy*

[c] *Euratom Association, Institut für Plasma Physik, FZ Jülich, Jülich, Germany*

Abstract

A fueling system by supersonic pulsed gas injection has been installed on the high field side of Tore Supra. First results are encouraging, demonstrating a fueling efficiency four times higher than that of conventional gas puff. One-dimensional modeling shows that the increase of efficiency is linked to the short injection time and to the prompt cooling of the plasma edge consecutive to the massive injection of matter. Improvements of the system could lead to the formation of a high-β blob which could experience a drift down the magnetic field, analogously to pellet injection, thus further increasing the fueling efficiency of the method.

PACS: 52.25.Ya; 52.40.Hf

Keywords: Plasma fueling; Supersonic gas injection; Particle diffusion; Recylcing; Tore Supra

1. Introduction

Efficient discharge fueling requires to deposit particles as deep as possible in the plasma, as the density is roughly proportional to the penetration of the injected matter. Two fueling methods are used routinely: gas puffing and pellet injection. Gas puffing is easy to implement, but has a poor fueling efficiency, the injected matter being deposited in the plasma periphery. Pellet injection is a far more complex system but has a much better fueling efficiency, depositing matter typically at mid radius. Moreover, the ablated material experiences $\mathbf{E} \times \mathbf{B}$ type drifts, due to charge separation phenomena. The first drift yields a poloidal rotation [1], the second, an outward radial drift down the magnetic field gradient, leading to enhanced matter penetration when injecting from the high field side [2]. The condition for these drifts to appear is a higher pressure in the blob of injected matter than in the background plasma [3].

To benefit from the radial drift described above, the supersonic pulsed gas injection (SPGI) consists in launching a very dense and short gas puff from the high field side. The advantage would then be the combination of an efficient fueling with a technology much simpler than for pellet injectors. Encouraging results have already been obtained on the Chinese tokamak HT-7 [4]. SPGI was tested on Tore Supra during the 2001 experimental campaign, demonstrating a fueling efficiency three to four times higher than for conventional gas puff (GP). These results are detailed in Section 2, where the experimental set up is described. The processes leading to the increase of the fueling efficiency are analysed in Section 3. The main results are discussed and summarized in Section 4.

2. Experimental set up and results

A supersonic gas injector has been installed in the equatorial plane on the high field side of Tore Supra

* Corresponding author. Tel.: +33-4 42 25 45 51; fax: +33-4 42 25 49 90.

E-mail address: pegourie@cea.fr (B. Pégourié).

0022-3115/03/$ - see front matter
PII: S0022-3115(02)01462-9

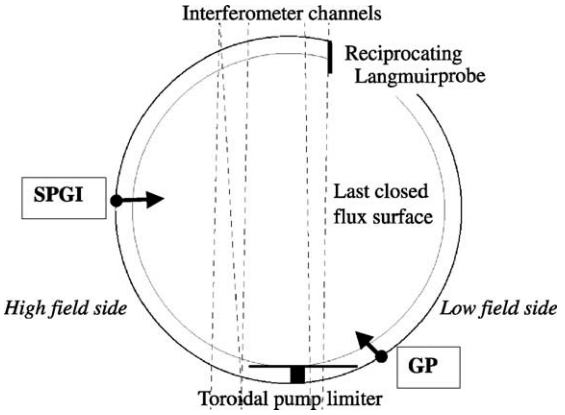

Fig. 1. Experimental set up, showing the nozzle location on the high field side, the TPL, the five chords for the line integrated density measurements and the reciprocating Langmuir probe trajectory.

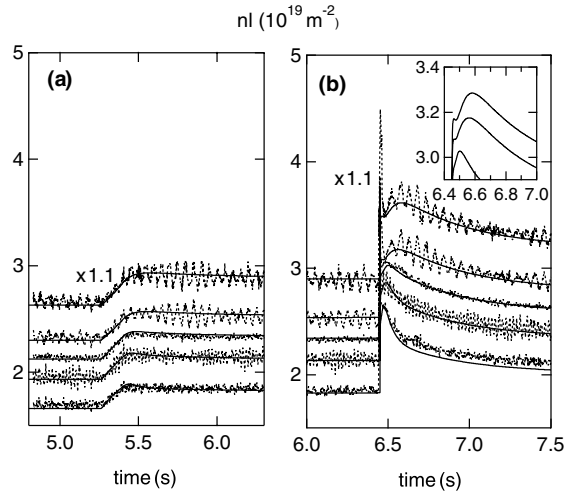

Fig. 2. Comparison between calculated and measured line integrated densities for GP (a) and SPGI (b). The upper curve is multiplied by 1.1 for clarity. The inset shows a detail of the simulation emphasizing the spike due to the recycling.

(Fig. 1), allowing to reach a Mach number up to 5, and to inject 0.4 Pa m^3 of D_2 molecules within 2–4 ms. This corresponds to injection rates up to 5×10^{22} part s^{-1}. A comparison of the line integrated density behaviour during GP and SPGI is shown in Fig. 2, the total number of particles injected being identical in both cases. Two successive injections were performed during the same L mode ohmic discharge, with no active pumping and with an average density of 1.6 and 1.8×10^{19} m^{-3}, respectively. The increase of density is moderate for GP, while for SPGI, a strong density rise is observed, with a first spike followed by a slower decay. A significant cooling of the plasma edge is observed (Fig. 6) generally yielding a transient detachment phase.

A database has been built for SPGI in terms of fueling efficiency $\varepsilon_{\text{fuel}}$ whose standard definition is the ratio of the increase of the plasma content divided by the number of injected particles just at the end of the gas injection. However, this cannot be used in our case, because the initial spike seen on the density measurements corresponds to a 3D structure whose toroidal and poloidal extensions are not known, which prevents to calculate the discharge particle content. Therefore, we used for the calculation of $\varepsilon_{\text{fuel}}$ the particle content 50 ms after the injection. The results are displayed in Fig. 3, where $\varepsilon_{\text{fuel}}$ is plotted as a function of the distance Δ between the injection nozzle and the plasma boundary (Fig. 3(a)), the line integrated density nl (Fig. 3(b)) and the number of injected particles N_{inj} (Fig. 3(c)). $\varepsilon_{\text{fuel}}$ ranges typically between 40% and 60% for SPGI (while it is 10–15% for GP and up to 80% for pellet injection). Although the data are scattered due to different plasma and injector conditions, the general trend is a decay with increasing Δ and nl, and a slight increase with increasing N_{inj}.

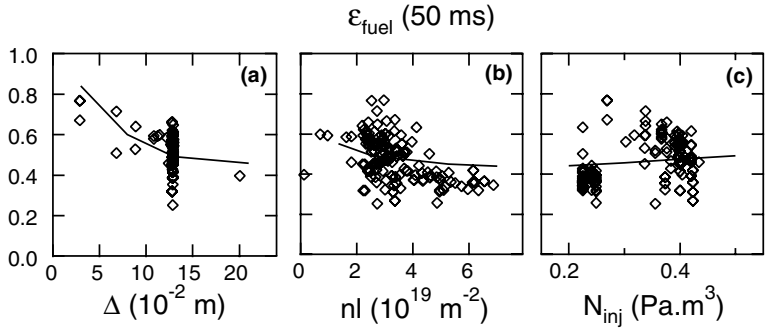

Fig. 3. Fueling efficiency of SPGI measured 50 ms after the end of injection vs. (a) the distance Δ between the nozzle and the LCFS, (b) the plasma line averaged density and (c) the number of injected particles. The lines are the model prediction.

3. Modeling of SPGI and conventional gas puff

The analysis starts from the cylindrical 1D continuity equation:

$$\frac{\partial n}{\partial t}+\frac{1}{r}\frac{\partial(r\Gamma)}{\partial r}=S-W, \tag{1}$$

where n is the density, Γ the radial particle flux, r the radial coordinate and S and W the particle source and sink respectively. In the confined plasma, $\Gamma=(-D\nabla+V)n$, where D is the diffusion coefficient and V the pinch velocity, and $W=0$. In the SOL, $\Gamma=-D\nabla n$ and $W=n/\tau_{\|}$ where the parallel SOL lifetime is given by $\tau_{\|}=2\pi qR_0/C_s$, q being the safety factor, R_0 the plasma major radius and C_s the sound speed.

In the SOL, the temperature is assumed to be exponential of e-folding length λ_T. At each time step, the temperature on the last closed flux surface (LCFS) is calculated assuming a constant conducted power P_{cond}:

$$P_{\text{cond}}=\frac{4\pi^2R_0\gamma}{g_{\|}}\int_{\text{SOL}}rW(r)T(r)\,\mathrm{d}r, \tag{2}$$

where $\gamma=7.8$ is the sheath transmission factor, and $g_{\|}=0.5$–0.3 the proportion of the total conducted power carried by the parallel flux [5].

Two sources of particles are considered: S_{ext} corresponds to the external feeding of the plasma by SPGI or GP, while S_{R} is the recycling source on the toroidal pumped limiter (TPL). The normalized profiles of S_{ext} and S_{R} are calculated with the 3D neutral code EIRENE [6], specifying in each case the characteristics of the molecular and/or atomic flow at the nozzle or on the TPL. The source $S_{\text{R}}=R\Gamma_{\text{out}}$ depends on both the plasma outflux Γ_{out} and wall recycling coefficient R. Experimentally, $R\approx 1$ before and after the injection since the plasma density is almost constant, and $R<1$ during the injection phase since the fueling efficiency is always lower than 100%. Practically, we use $R=1$ except during the injection phase where R is adapted to fit the time behaviour of the measured H_α (Fig. 4). Satisfactory fits of the whole data set are obtained for R between 0.6 and 0.8. Initial conditions of the calculation are given by the five pre-injection line-integrated densities and measured SOL characteristics. The profile of the D/V ratio is constrained by the initial density, the absolute values for D and V being then chosen so that the particle lifetime τ_{p} is consistent with values reported in [7] ($\tau_{\text{p}}=N_{\text{tot}}/\Gamma_{\text{out}}$ where N_{tot} is the total number of particles in the discharge). For long times, S_{R} is increased by 8% to fit the new equilibrium density. The experimental values of P_{cond}, τ_{p}, SOL characteristics and resulting transport coefficients are listed in Table 1. The normalized particle source profiles S_{R} and S_{ext} (SPGI and GP), calculated with the pre-injection plasma profiles, are shown in Fig. 5(a). For comparison, S_{R} and S_{SPGI} at the time of maximum SOL cooling are presented in Fig. 5(b). Even though the penetration is slightly increased in the cold plasma case, the particle sources still remain peripheral.

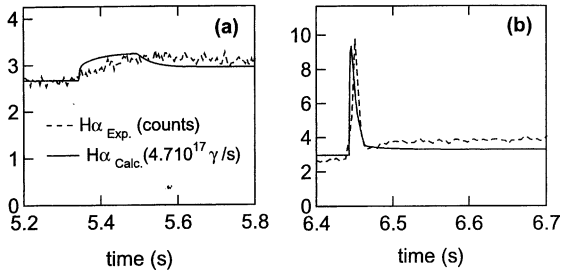

Fig. 4. Measured and calculated H_α emission of the recycling on the TPL using an adjusted recycling coefficient during the gas injection phase to reproduce the experimental data. (a) GP, (b) SPGI.

The SPGI and GP can then be simulated by putting in the above model the appropriate external source S_{ext} (Fig. 5) and injection time τ_{inj}, with $N_{\text{inj}}=S_{\text{ext}}\tau_{\text{inj}}=0.42$ Pa m^3 in both cases $\tau_{\text{inj}}=2$ ms for SPGI, 150 ms for GP). The transport parameters are identical for both cases and kept constant during the simulation. The measured and simulated line integrated densities are compared in Fig. 2 for SPGI and GP. The agreement is satisfactory for both cases, the only feature not reproduced being the spike at the injection time for SPGI. Due to the large difference in the injection times, the behaviour of the line density for SPGI is much closer to the impulse response of the system than in the case of GP (i.e. $\tau_{\text{inj}}\ll\tau_{\text{p}}$ for SPGI while $\tau_{\text{inj}}\geqslant\tau_{\text{p}}$ for GP). According to the modeling and with the used transport parameters, the additional process leading to a further increase of $\varepsilon_{\text{fuel}}$ of SPGI is not a deeper matter deposition (which remains peripheral, see Fig. 5), but the rise of the lifetime $\tau_{\|}$ of the particles in the SOL, due to the

Table 1
Experimental and calculated plasma and SOL characteristics and transport coefficients (see [8] for an overview of the particle transport coefficients in Tore Supra)

	P_{cond} (MW)	τ_{p} (ms)	n_{LCFS} (10^{18} m^{-3})	λ_n (cm)	T_{LCFS} (eV)	λ_T (cm)	$D(a/2)$ (m^2/s)	V_{LCFS} (m/s)	$\tau_{\|}(t=0)$ (ms)
Experiment	0.33	120–170	2.5–3.0	4	50–55	5	–	–	–
Simulation	0.31	135	2.5	2–4	55–60	5	0.4	−5.7	1–4

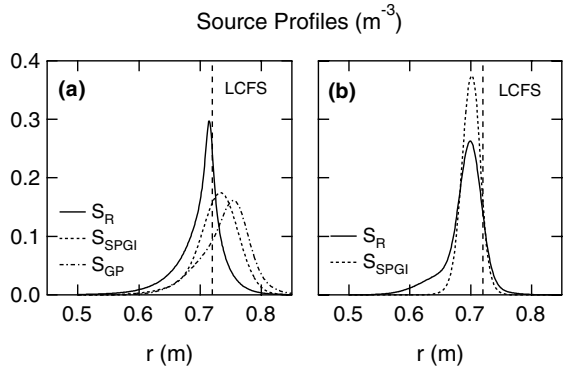

Fig. 5. S_R and S_{ext} normalized profiles vs. minor radius. Also shown is the LCFS at $r = 0.72$ m. (a) Pre-injection plasma conditions, (b) time of maximum SOL cooling during SPGI.

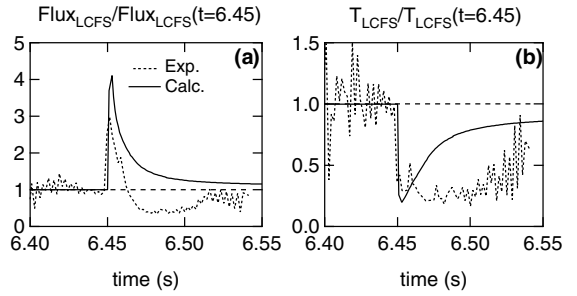

Fig. 6. Ratio of (a) the parallel particle flux and (b) the SOL temperature at the LCFS during and before (at $t = 6.45$ s) SPGI, showing the flux rise and the temperature drop due to the injection. Shown are the experimental measurement from the reciprocating probe and the values calculated by the model.

cooling of the plasma linked to the massive injection of matter for SPGI. In particular, drifts increasing the effective penetration of the matter are not needed to reproduce the experimental line densities. The plasma cooling is illustrated in Fig. 6 where the calculated and measured temperature and flux variations during SPGI are compared. The initial phase is correctly reproduced while a significant discrepancy appears for longer times. This is due to the assumption of constant conducted power in the modeling, which is not verified in the experiment where SPGI is followed by a phase of about 100 ms during which the plasma is semi-detached. The spike observed on the line integrated densities can be attributed to the recycling of the matter ionized close to the LCFS and transported to the limiter immediately after the injection. In the simulations, this first phase is seen with the correct time scale (see inset of Fig. 2(b)) but the amplitude of the peak is not reproduced. This is due to the 1D modeling approach where all the sources are averaged in the poloidal and toroidal directions, while the recycling on the TPL is essentially a 2D pattern. Finally, the model predictions have been compared to the database displayed in Fig. 3(a)–(c), showing the right trend.

4. Discussion and summary

If SPGI has been demonstrated to be an efficient fueling method (efficiency in the range 30–60%, i.e. three to four times that of GP), better performances are yet possible since no cold material drift down the magnetic field gradient has been evidenced so far. Indeed, analysis using a diffusion model with realistic particle sources has shown that the short injection time and the prompt cooling of the plasma edge consecutive to the massive injection of matter was sufficient to explain the good efficiency of the method. The actual control parameter is therefore the instantaneous strength of the particle source. For a fixed quantity of injected matter, a shorter injection time would then increase the pressure in the blob of cold material and might trigger the drifts mentioned above. An upgraded supersonic injector is presently under development. To assess the suitability of such a system for fueling next step devices, major points still remain to be investigated: the effect of the strong perturbation of the edge of the discharge by SPGI on H-mode plasmas performances and on the coupling of the RF heating systems.

References

[1] B. Pégourié, J.-M. Picchiottino, Phys. Plasmas 3 (1996) 4594.
[2] P.T. Lang, K. Büchl, M. Kaufmann, R.S. Lang, et al., Phys. Rev. Lett. 79 (1997) 1487.
[3] V. Rozhansky, I. Veselova, S. Voskoboynikov, Plasma Phys. Control. Fusion 37 (1995) 399.
[4] X. Gao et al., Phys. Plasmas 7 (2000) 2933.
[5] R. Mitteau, J.C. Vallet, A. Moal, D. Guilhem, et al., Heat flux pattern on the toroidal pump limiter of Tore Supra: first observations and preliminary analysis, these Proceedings.
[6] D. Reiter, The EIRENE code, version: Jan. 92 – Users manual, Technical report Jül-2599 KFA-Jülich, 1992, see also www.eirene.de.
[7] E. Tsitrone, PhD thesis, Contrôle des flux de particules dans un tokamak au moyen d'une structure à évents, Université de Provence Aix-Marseille I, 1995.
[8] P. Laporte, T. Hutter, J.C.M. de Haas, H. Capes, in: 21st EPS Conference on Controlled Fusion and Plasma Physics, vol. 18B-I, EPS, 1994, p. 62.